Tundra vegetation community, not microclimate, controls asynchrony of above and belowground phenology

Abstract:

The below-ground growing season often extends beyond the above-ground growing season in tundra ecosystems. However, we do not yet know where and when this occurs and whether these phenological asynchronies are driven by variation in local vegetation communities or by spatial variation in microclimate. Here, we combined above- and below-ground plant phenology metrics to compare the relative timings and magnitudes of leaf and root growth and senescence across microclimates and plant communities at five sites across the tundra biome. We observed asynchronous growth between above-ground and below-ground plant tissue, with the below-ground season extending up to 74% beyond the onset of above-ground leaf senescence. Plant community type, rather than microclimate, was a key factor controlling the timing, productivity and growth rates of roots, with graminoid roots exhibiting a distinct 'pulse' of growth later into the growing season than shrub roots. Our findings indicate the potential of vegetation change to influence below-ground carbon storage as roots remain active in unfrozen soils for longer as the climate warms. Taken together, increased root growth in soils that remain thawed later into the growing season, in combination with ongoing tundra vegetation change including increased shrubs and graminoids, can act together to alter below-ground productivity and carbon cycling in the tundra biome.

Authors and affiliations

- **Corresponding author:** Elise Gallois elise.gallois@nhm.ac.uk. (0000-0002-9402-1931). 1) University of Edinburgh, Address: The King's Buildings, Alexander Crum Brown Road, Edinburgh EH9 3FF. 2) Natural History Museum Address: Cromwell Rd, South Kensington, London SW7 5BD.
- Isla Myers-Smith (0000-0002-8417-6112), Department of Forest and Conservation Sciences, Faculty of Forestry, University of British Columbia, Global Change Research Institute, School of GeoSciences, University of Edinburgh
- Colleen Iversen (0000-0001-8293-3450), Environmental Sciences Division, Oak Ridge National Laboratory, Oak Ridge, 37831, TN, USA.
- Verity Salmon (0000-0002-2188-551X), Environmental Sciences Division, Oak Ridge National Laboratory, Oak Ridge, 37831, TN, USA.
- Laura L Turner (0000-0002-5254-2106), School of Geography, The University of Nottingham, University Park, Nottingham, NG7 2RD.
- Ruby An (0000-0002-5339-2242), Princeton University, 106A Guyot Hall, Princeton University, Princeton, NJ 08544-2016 U.S.A.
- Sarah C. Elmendorf (0000-0003-1085-8521). (1) Institute of Arctic and Alpine Research, University of Colorado, Boulder CO USA. (2) Department of Ecology and Evolutionary Biology. University of Colorado, Boulder CO USA.
- Courtney G. Collins (0000-0001-5455-172X). 1)Biodiversity Research Centre, The University of British Columbia, Vancouver, BC, Canada, 2) Department of Botany, The University of British Columbia, Vancouver, BC, Canada.
- Madelaine Anderson (0000-0001-6571-9620), Département de Biologie, Université de Sherbrooke, Sherbrooke, QC, J1K 2R1, Canada
- Amanda Young (0000-0002-3580-8603), Toolik Field Station, Institute of Arctic Biology, University of Alaska Fairbanks, Fairbanks, AK 99775
- Lisa Pilkinton, University of Edinburgh, Address: The King's Buildings, Alexander Crum Brown Road, Edinburgh EH9 3FF
- Gesche Blume-Werry (0000-0003-0909-670X), Department of Ecology and Environmental Science, Umeå University, Umeå, Sweden
- Maude Grenier (0000-0002-3153-0616), UK Centre for Ecology and Hydrology, Edinburgh Research Station, Penicuik, EH26 0QB, UK.
- Geerte Fälthammar de Jong (0000-0003-3774-1059), University of Gothenburg, Medicinaregatan 7 B, 41390 Göteborg, Sweden
- Inge H.J. Althuizen (0000-0003-3485-9609 1) NORCE Norwegian Research Centre AS, Bergen, Norway 2) Bjerknes Centre for Climate Research, Bergen, Norway
- Casper T. Christiansen, (0000-0002-4526-614X), Terrestrial Ecology Section, Department of Biology, University of Copenhagen, Copenhagen, Denmark
- Simone I. Lang (0000-0002-6812-2528), The University Centre in Svalbard, Postboks 156, 9171 Longyearbyen, Norway
- Cassandra Elphinstone (0000-0002-2968-1431), Department of Botany, University of British Columbia, 6270 University Blvd, Vancouver, BC V6T 1Z4, Canada.
- Greg Henry (0000-0002-2606-9650), Department of Geography, University of British Columbia, Vancouver, BC V6T 1Z4, Canada.
- Nicola Rammell (0000-0002-3536-298X), Department of Geography, University of British Columbia, Vancouver, BC V6T 1Z4, Canada.
- Michelle C. Mack (0000-0003-1279-4242), Institute of Arctic Biology, University of Alaska, Fairbanks, 99775, Alaska, USA
- Craig See (0000-0003-4154-8307), Center for Ecosystem Science and Society, Northern Arizona University, Flagstaff, Arizona, USA

87   • Christian Rixen (0000-0002-2486-9988). 1) WSL Institute for Snow and Avalanche Research
88   SLF, Davos, Switzerland, 2) Climate Change, Extremes and Natural Hazards in Alpine
89   Regions Research Centre CERC, Davos Dorf, Switzerland
90   • Robert Hollister (0000-0002-4764-7691), Grand Valley State University.1 Campus Dr.
91   Allendale, MI 49401
92
93

Introduction

Over the last three decades many tundra plants have exhibited earlier phenology in response to warmer summer temperatures, and at a rate of change higher than in the planet's more temperate regions (Høye et al., 2007; Panchen & Gorelick, 2015, 2017; Prevéy et al., 2019; Wookey et al., 1993). Above-ground (*leaf, shoot, and flower*) phenology varies in timing and in strength of sensitivity to local abiotic drivers (such as snowmelt and surface temperature) and by species (Assmann et al., 2019; Bjorkman et al., 2015; Prevéy et al., 2017). In Arctic Sweden and Western Greenland, the timing of above- and below- ground plant growth has been observed to be asynchronous, with the below-ground growing season extending up to 50% longer than the above ground growing season (Blume-Werry, 2021; Blume-Werry et al., 2016; Liu et al., 2021; Radville et al., 2016; Sullivan et al., 2007). In addition, below-ground root growth has been found to be relatively unresponsive to experimental manipulations of temperature and snowmelt timing (Blume-Werry et al., 2017). However, previous studies have not tested the asynchrony and drivers of above- *versus* below-ground root productivity and the timing of root growth across tundra sites and throughout tundra landscapes across microclimates.

Belowground plant biomass represents 24% of overall global average plant biomass (Ma et al., 2021), yet in much of the tundra biome approximately 80% of vegetative biomass is found belowground (Mokany et al., 2006). Tundra plants have the shallowest roots among all of the world's biomes and are adapted to be highly productive despite the high permafrost table and cold soil conditions (Iversen et al., 2015; Schenk & Jackson, 2002; Shaver & Billings, 1975). However, the below-ground component of tundra ecosystem dynamics remains a 'black box' (Iversen et al., 2015). Root growth patterns and phenological dynamics are critically under-represented in terrestrial ecosystem and carbon models due to scarcity of data and oversimplification of root-microenvironment relationships (Smithwick et al., 2014; Warren et al., 2015). Plant roots efficiently convert atmospheric carbon into stable soil carbon (Jones et al., 2009; Sokol & Bradford, 2019) and are a large source of decomposable litter, much of which is respired back into the atmosphere (Sullivan et al., 2007; Zona et al., 2022). However, our understanding of the physiological coupling of above- and below-ground phenology and the abiotic drivers of tundra root growth remain limited, hampering our ability to accurately model tundra ecosystem carbon cycling in tandem with climate warming (Smithwick et al., 2014; Warren et al., 2015).

Plant productivity, aboveground biomass, and shrub and graminoid abundance are increasing across multiple Arctic and alpine tundra field sites in concert with climate warming (Berner & Goetz, 2022; Bhatt et al., 2013; Elmendorf et al., 2012; Forbes et al., 2010, 2010; Myers-Smith et al., 2011, 2020). Much of this change is specifically attributed to the encroachment and subsequent range expansion of woody shrubs, including increases in both height and breadth of individual shrubs (Forbes et al., 2010; García Criado et al., 2020; Martin et al., 2017; Naito & Cairns, 2011; Tape et al., 2006). Graminoid species are also expected to increase in abundance in response to climate change (Bjorkman et al., 2020; Elmendorf et al., 2012) and through local phenomena such as flooding or water-logging via permafrost thaw (Heijmans et al., 2022). While there is ample evidence of regional- and local-scale tundra ecosystem change based on long-term observations of above-ground tundra vegetation, below-ground biomass and phenology change is much more challenging to track and thus rarely reported (Iversen et al., 2015).

Different plant functional types have different root growth strategies, and thus any future vegetation range shifts may have important ecological consequences in tundra soils. The ways in which roots grow, acquire and use nutrients and interact with biotic stimuli vary considerably between plant functional types in tundra soils (de Kroon et al., 2012). For example, shrubs often root earlier in summer and in shallower soils while graminoids often root later in summer and in deeper soils near the thaw front (Keuper et al., 2017; McKane et al., 2002; Schwieger et al., 2018; Sullivan et al., 2007). Increased root production in warmer soils could provide more efficient mechanisms of stable sequestration of atmospheric carbon (i.e., Sokol & Bradford, 2019), but could also lead to greater long term loss in soil organic carbon through increased decomposition of root litter particularly for sedge species with annual root turnover (i.e., Sullivan et al., 2007). Long-term vegetation changes in response to a warming climate may also be influenced by competitive advantages belowground, for example species able to forage deeper and for longer in permafrost soils may benefit as permafrost soils thaw (Hewitt et al., 2019; Pedersen et al., 2020)21/06/2024 13:17:00, while the expansion of some species may be promoted by the climate-enhanced development of ectomycorrhizal networks (Deslippe et al., 2011). Quantifying rooting phenology strategies across microclimates and plant communities will allow us to predict future changes in belowground growth patterns and changes in carbon and nutrient cycling dynamics in warming tundra ecosystems (Smithwick et al., 2014; Warren et al., 2015).

162

Above-ground productivity and phenology are influenced by both macro- and micro-environmental variables, including snowmelt timing and soil, surface, and air temperatures (Assmann et al., 2019; Høye et al., 2007; Panchen & Gorelick., 2015; Wookey et al., 1993), yet these same drivers may have less influence below-ground (Abramoff & Finzi, 2016; Liu et al., 2021). Experimental warming studies at tundra sites have indicated that the duration of root growing seasons for some species are largely unresponsive to factors that influence aboveground phenology, such as snowmelt timing or warming (Möhl et al., 2022). However, while the overall length of the belowground growing season may not change, the timing of peak root growth may be shifted, for example to later in deeper and warmer soils as permafrost thaws (Blume-Werry et al. 2019). Thus, root phenology may be influenced to some degree by late-season timings of permafrost thaw, in particular for those species able to forage deeper to access the active layer thaw front (Blume-Werry et al., 2019; Hewitt et al., 2019; Salmon et al., 2018). Variation in temperature across heterogeneous landscapes in a space-for-time setup could inform our understanding of change over time with warming (Ma et al., 2022; Radville et al., 2018; Schwieger et al., 2018).

178

Abiotic (air temperature and thaw depth) and biotic (nutrient hormone allocation) controls may differ between above- and below-ground plant tissue (Abramoff & Finzi 2015, Liu et al. 2021, Ma et al 2022). However, we lack paired above- and below-ground phenology observations across vegetations types and local temperature variation to test the extent to which these drivers are decoupled. Here, we combined leaf phenology observations with root growth metrics collected across five tundra sites and 39 individual plots to compare the relative timings of plant tissue growth and senescence in both the above- and below-ground environment. We analysed root growth patterns across locally-varied temperature gradients to determine how root growth varies across warmer versus colder belowground conditions across the growing season. We also investigated root growth dynamics across graminoid- *versus* shrub-dominated plant communities to quantify different root phenological strategies between two dominant tundra plant community types. Analysing different root and leaf phenology across microclimates provides a useful space-for-time comparison whereby warmer areas, in comparison to cooler areas, act as a natural proxy for future climate warming. Analysing root growth patterns between community types will inform how tundra vegetation change could influence below-ground root productivity, dynamics and ultimately carbon cycling (Bjorkman et al., 2020; Heijmans et al., 2022; Myers-Smith et al., 2011; Niittynen et al., 2020).

196

In this study, we address the following research questions:

198

RQ1. (Above- and below-ground): Is there above- *versus* below-ground asynchrony in phenology, and how does it vary across microclimates and community types? Site-specific studies indicate that the below-ground growth of tundra plants extends beyond the period of growth above ground (Blume-Werry, 2021; Blume-Werry et al., 2016; Radville et al., 2016). Therefore, we predict that root growth will continue accumulate as the leaf tissue above-ground is senescing and that this asynchrony will be greater in warmer microclimates versus colder microclimates. At sites with permafrost, if deeper active layers increase the overall volume of available soil in which roots can grow throughout the growing season, root growth could be greater in warmer microclimates. There may be a lag between above-ground phenology and below-ground phenology because soil temperatures lag behind air temperatures and thaw progressively across the summer, which may influence the timing of root production and foraging. If asynchrony is detected but is not explained by local temperature variation, plant community type could be the primary driver, particularly if there is clear differentiation in rooting strategy between plant functional types.

213

RQ2. (Below-ground only): Is root productivity higher and the period root growth longer in warmer versus cooler parts of the landscape? Microclimates influence the growth of tundra plants, with greater productivity in warmer versus colder microclimates (e.g., Blume-Werry, 2021; Liu et al., 2021). Thus, we predict that there will be higher fine root production in the warmer versus cooler parts of the landscape, leading to higher biomass in the warmer plots within each site (e.g., Sullivan et al., 2007). We expect that root growth will extend for longer in the warmer versus cooler plots within each site.

221

RQ3. (Below-ground only): How does plant community type control below-ground plant biomass and phenology? Different plant functional types have different root growth strategies and can exhibit differentiating timing of root foraging to acquire water and nutrients from permafrost soils (e.g., de Kroon et al., 2012; Pedersen et al., 2020). For this reason, we predict that graminoid-dominated communities will exhibit root growth later in the season than shrub-dominated communities as they are deeper-rooting and may grow later in the season to access nutrients released later in the summer by thawing permafrost.

229

Methods

Site Selection

We studied five tundra biome sites including Arctic tundra (Toolik Lake, Alaska, USA), Subarctic alpine tundra (Kluane Lake, Yukon, Canada) and high latitude alpine tundra (BC Coastal Mountains, BC, Canada; Niwot Ridge, Colorado, USA; Cairngorms Mountains, Scotland, UK). These sites span a wide geographical and climatological range (**Fig. 1**; **Table S1**). Each site also spans a range of microenvironmental gradients and includes a combination of graminoid-dominated, shrub-dominated and mixed-species communities, which we classified using site-specific metadata, *in-situ* observations, and phenocam observations (**Table S1**). Each site was outfitted with in-growth cores with a paired TOMST environmental logger, and all sites had phenocams installed.
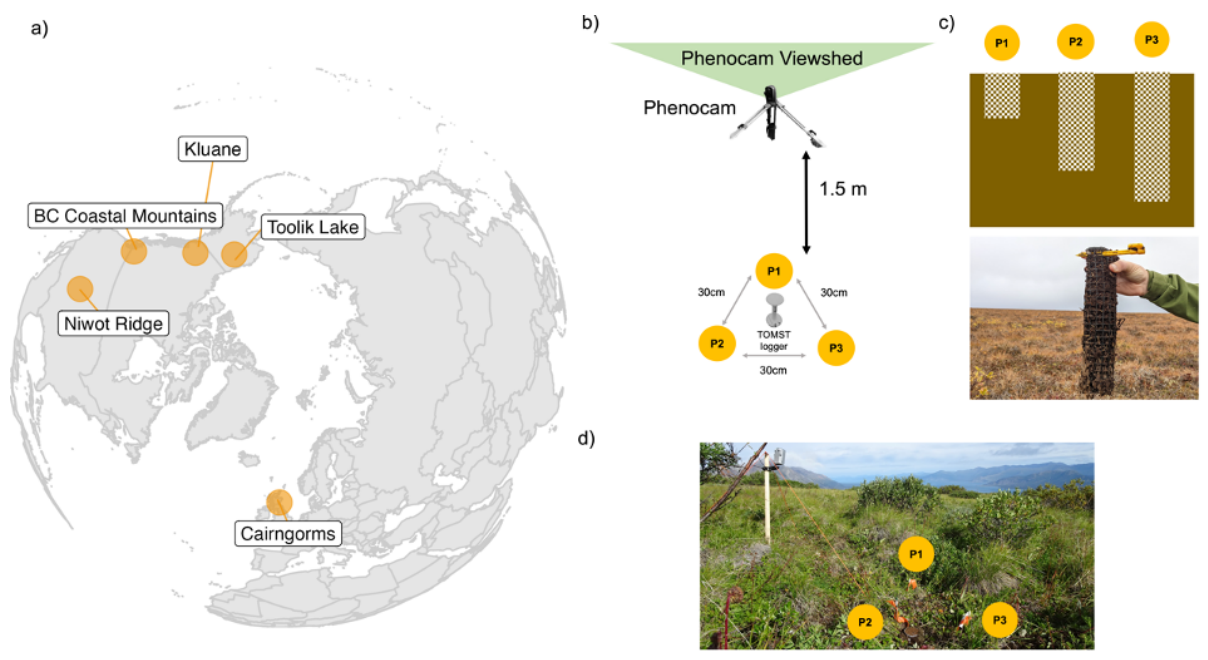
Figure 1. Our study includes five sites and subplots containing paired phenocams and in-growth cores. a) Polar projection map of the five Arctic, subarctic and alpine tundra sites included in this study. b) Birds-eye-view schematic of the subplots, showing the location of in-growth cores P1, P2 and P2 in relation to the phenocam and the TOMST microclimate logger. c) Cross-section schematic of the differential in-growth core depths in the soil profile at sites with permafrost (sites without permafrost had the same depth for all cores). Photograph of a P3 core removed from Toolik Lake in 2022 (Image Credit: Ruby An). d) Photograph of Kluane

Subplot 8 with a phenocam pointed northwards, alongside three buried in-growth cores in summer 2021 (Image Credit: Madeleine Anderson).

In-Growth Core Construction

The observation tools most commonly used in below-ground phenology studies (minirhizotrons) cannot be easily installed in Arctic and alpine tundra dominated by permafrost as the tubes can be pushed upwards due to freeze-thaw dynamics, and therefore we elected to use an in-growth soil core field approach. We constructed in-growth peat cores with a 7 cm diameter using plastic meshing (rigid garden netting or industrial mesh tubing) with mesh holes no wider than 1 cm x 1 cm diameter. Each core was filled with sterilised milled peat from garden centres local to the study sites (**Table S1**). We packed the milled peat into the in-growth cores tightly to achieve similar densities between cores. At sites with permafrost (**Table S1**), in each cluster of three cores (hereafter, *plot*), the cores were divided into lengths of 10 cm (Phenology 1, or 'P1'), 20 cm (Phenology 2, or 'P2'), 30 cm (Phenology 3, or 'P3'). These different core lengths accounted for the differing active layer depths across the growing season in the summer of core removal such that the P1 cores could be removed early in the growing season when the permafrost active layer was theoretically closer to the surface. At sites without permafrost (**Table S1**), all cores had the same depth based on the soil depth at each site (between 15-20 cm). We recorded the weight and length of the cores at each site prior to deployment in the field.

Core Installation

At each site in the summers of 2021 and 2022, we separated the cores into clusters (one cluster = one x P1, one x P2, one x P3) and chose site locations whereby a minimum of five plots (15 cores in total) were distributed along environmental gradients specific to those sites, including soil moisture gradients, shrub versus graminoid-dominated communities, and elevational gradients. We recorded the geographic location of each site/plot using equipment available to contributors across sites. The core installation process took place at the end of the growing season at all sites to ensure limited root growth in the year of installation.

At each plot, the three cores were buried 30 cm away from one another in a triangular arrangement (see **Fig. 1**). Using a soil auger, we took a core of up to 30 cm depth (depending on the phenology classification of the core; i.e., P3) and recorded from this core the depth (cm) from the top of the core from at which the organic material transitions to a sandy or silty layer,

286 a qualitative description of the soil type and density (e.g., 'loose loamy' or 'dense clay'), and

287 the depth (cm) from the top of the core of maximum rooting. We gently placed the peat-filled

288 in-growth cores into the boreholes, making sure the base of the core reached the bottom of the

289 hole and that there was no mesh extending upwards from the surface of the hole.

290

291 At each plot, we labelled the cores with a unique ID on a small flag or stake. In the centre of

292 each plot, we installed microclimate loggers (**Table S1**) which logged temperature at -6, +2

293 and +15 cm from the surface (TMS) or 0 cm from the surface (HOBO Pendant) over the course

294 of the experiment. For each of the sites, we reclassified the raw surface temperature data into

295 quantiles (hereafter 'temperature quantiles') to generate even and comparable groupings of the

296 relative coldest-Q1, cool-Q2, warm-Q3, and warmest-Q4 areas across the landscape at each

297 site (**Table S1**). We intended initially to use soil temperature (-6 cm) data to better represent

298 belowground climate conditions. However, the soil temperature readings were corrupted at

299 some plots in two (Toolik Lake, Niwot Ridge) of the five sites, so we used July and August

300 surface temperature (+2 cm) for consistency across sites and microclimate datasets.

301

302 *Phenocam Installation*

303 At the sites (**Fig. 1, Table S1**), we installed time lapse cameras (Moultrie Wingscape

304 TimelapseCam Pro) at the location of each plot where possible. We affixed the phenocams to

305 sturdy metal tripods at a height of 1 m above the ground. The phenocams pointed northwards

306 to avoid direct sunlight and prevent glare, allowing the cameras to capture snow melt timing

307 and the landscape greenness over the course of the growing season. We set the cameras to

308 infinite focus and set to capture one photograph per hour or four photographs per day at the

309 highest pixel resolution possible for each camera. We installed these phenocams in 2021 when

310 burying the cores, programmed them to collect imagery over the winter and following summer,

311 and downloaded the data at the end of the growing season once the last core (P3) had been

312 removed from each plot.

313

314 *Core Removal*

315 The summer following core installation (i.e., 2022 when cores were installed in 2021), we

316 removed the cores from the plots at staged intervals. We collected the P1 cores at the beginning

317 of the growing season (shortly after snowmelt), the P2 cores at the middle of the growing

318 season (corresponding with peak aboveground productivity), and the P3 cores at the end of the

319 growing season (before the return of snow). Due to logistical constraints and site-specific

productivity differences, the removal dates varied across sites but were consistent within sites. During the 2022 field season, we used soil moisture probes to once again record the soil moisture content (%) at each of the plots. In addition, the temperature logger data and phenocam images were downloaded at the end of the growing season. Upon removal, the cores were immediately frozen to prevent root rot, and at the end of the growing season all cores were shipped to the University of Edinburgh for laboratory analysis.

Laboratory Analysis

After thawing each of the frozen cores for 24 hours in a refrigerator, we sub-sectioned each core into distinct depth increments from surface to base (0-5 cm, 5-15 cm, 15-25 cm and 25-30 cm as appropriate for overall length). We recorded the full weight of each core, and the full weight of each of these subsections. In addition, we recorded the weight of a wet soil subsample from the 0-5 cm increment of each core before drying them in an oven at 60°C for 72 hours, and then recording the weight of the dried subsamples. We used the difference between these two weights to calculate the bulk densities of each of the depth increments, whereby;

Equation 1a

$$BD_{wet} = W / V$$

$$BD_{wet} = wet\ weight\ bulk\ density$$
$$W = wet\ weight\ of\ ingrowth\ core\ depth\ increment$$
$$V = cylindrical\ volume\ of\ ingrowth\ core\ depth\ increment$$

Equation 1b

$$BD_{dry} = BD_{wet} * (W_{ds} / W_{ws})$$

$$BD_{dry} = dry\ weight\ bulk\ density$$
$$W_{ds} = dry\ weight\ of\ soil\ subsample$$
$$W_{ws} = wet\ weight\ of\ soil\ subsample$$

For each depth increment, we used tweezers to extract all of the roots within the soil, and used distilled water to clean off the excess peat. We separated the roots into petri-dishes based on

morphological and colour differences. Once cleaned and separated by group and depth increment, we scanned each of the root groups using an Epson Perfection V850 scanner with an inbuilt wet tray, in 16-bit grayscale and using an 800 dpi resolution. After scanning each root type by depth increment, we then placed the roots in metal tins and dried them in an oven at 60°C for 72 hours, and then recorded the weight using a fine scale.

We summed the overall root biomass for each depth increment, before calculating root biomass density (i.e., root biomass per unit soil volume g cm^{-3}, see: Freschet et al., 2021). We calculated a daily root growth rate over the course of the growing season for each plot using the following equation:

Equation 2

$$R = \frac{P3_{rd} - P1_{rd}}{P3_{doy} - P1_{doy}}$$

$$R = Root\ biomass\ growth\ rate$$
$$P3_{rd} = Root\ biomass\ per\ unit\ of\ dry\ bulk\ density\ for\ P3\ ingrowth\ core$$
$$P1_{rd} = Root\ biomass\ per\ unit\ of\ dry\ bulk\ density\ for\ P1\ ingrowth\ core$$
$$P3_{doy} = Day\ of\ year\ of\ P3\ in-growth\ core\ removal$$
$$P1_{doy} = Day\ of\ year\ of\ P1\ in-growth\ core\ removal$$

Cores varied in length across sites due to site-specific differences (i.e., soil quality, depth, presence or absence of permafrost) and in timing of extraction (due to the timing of site-specific permafrost thaw, snow melt and snow return). To examine the differences between whole-core root biomass versus distinct sections of the soil depth profile, we plotted average root density for the full cores to compare against the average root density from only the top 5 cm of the cores (**Fig. S2**) and ran alternate versions of the statistical analysis using data from just the top 0-5 depth increments of each of the cores (**Table S3**). In this article, we present both sets of results, but focus on the whole-core data because these data better capture the full rooting depth of each sample (see: Freschet et al., 2021).

Phenocam Analysis

We sequentially manually browsed phenocam images for each plot and recorded the day-of-year for the first occurrence of the following phenophases: plants first visible through snow,

90% snow melted, first 100% snow-free day, first green leaf, 50% leaves green, 100% leaves green, first senesced leaf, 50% leaves senesced, 100% leaves senesced, first end-season snow return, 50% end-season snow cover, 100% end-season snow cover. We made these observations at the community level (i.e., the across the entire viewshed of the phenocam) instead of recording the phenophases of individual plants of select species to ensure consistency of approach across all sites, and to generate proxies of greenness that we could use to interpret above-ground productivity and the timing of both green-up and senescence.

We used a combination of phenocam imagery, metadata from collaborators, and scanned root images to qualitatively classify the plots into graminoid-dominated, shrub-dominated, or mixed-species community groupings. Finally, we calculated a "synchrony metric" for each core cluster to estimate the percentage of total root growth that had occurred per plot between the first in-growth core removal date (P1) and the date of peak aboveground growth for each plot, relative to the maximum root growth from stage P3. This metric represents a coarse estimate of root growth accumulation by the time of peak above-ground greenness relative to the total root accumulation observed in the P3 cores (see **Fig. S1**). Therefore, the metric is more comparable within sites (i.e., all of the P1 and P3 removal dates are consistent at each location), but is not as comparable across sites (i.e., P1 and P3 removal dates will vary between, for example, Toolik Lake and Niwot Ridge).

Equation 3:

$$S = (((PG_{doy} - P1_{doy}) * R) / P3_{rd}) * 100$$

$S = Synchrony\ Metric = \%\ Root\ Growth\ at\ date\ of\ 100\%\ Greening$

$PG_{doy} = Day\ of\ year\ of\ peak\ aboveground\ growth\ (i.e.\ 100\%\ living\ leaves\ in\ plot\ green)$

$P1_{doy} = Day\ of\ year\ of\ P1\ in-growth\ core\ removal$

$P3_{rd} = Root\ biomass\ per\ unit\ of\ dry\ bulk\ density\ for\ P3\ ingrowth\ core$

$R = Root\ biomass\ growth\ rate\ (accounting\ for\ P1\ to\ P3\ growth\ rate)$

We also calculated specific P1-P2 and P2-P3 root growth rates to distinguish any accelerations between time periods. However, due to the differential timing of P2 removals across sites (i.e., the removals were not always exactly mid-season) we chose not to include these in any statistical analyses, but have instead visualised the results in **Figure S4**.

Statistical Analysis

We used Bayesian linear models to run three sets of regression analysis: 1) one set examining the variation of root biomass across microclimates and plant communities, 2) one set examining the variation in root growth rates across microclimates and plant communities, and 3) one set examining the variation of our derived synchrony metric across microclimates and plant communities. We square-root transformed the root biomass density data to fit a gaussian distribution. For each model we included 'community type' and 'microclimate quantile' as categorical fixed effects, and for the biomass model alone we included the removal stage (P1, P2, P3) as a categorical fixed effect to examine the differences in root biomass development across in-growth core removal intervals. Microclimate and community type do not co-vary strongly at these sites (**Fig. S3**).

To account for differences in environmental characteristics and in-growth core materials used between sites, we included "site" as a random intercept term. We intended to include random slopes in the model design to allow for different relationships between root phenology variables and the fixed effects, but ultimately removed this model structure due to lack of model convergence. We used the '*brms*' package (Bürkner, 2017) in *R* version 3.6.3 (R Core Team, 2013) and fitted each of the models with weakly informative priors (half Student-t priors with three degrees of freedom), with three chains of 4000 iterations each and a warmup of 1000 iterations. To assess model convergence, we examined Bayesian trace plots and posterior predictive fits, and checked to ensure that R_{hat} values (ratio of effective sample size to overall number of iterations) were all close to 1.00.

Results

We found that root growth continued for at least 56 days (on average) after the date of peak above-ground productivity at each site (**Fig. 2**). These root growth timings are under-estimates, as we did not collect any additional belowground data before the start, and beyond the end of our respective field expeditions. Calculated as the period of time relative to the first date of above-ground leaf yellowing, root biomass continued to increase for at least 62 days (or 74%) after the onset of above-ground senescence at Toolik Lake, 32 days (64%) in the BC coastal mountains, 60 days (47%) at Niwot Ridge, and 101 days (48%) in the Cairngorms. Meanwhile

there was no detectable increase in root biomass over time at Kluane Lake, potentially due to the scarcity of core extractions during the above-ground senescence period (**Fig. 2**). Across sites, we did not find any difference between above- and below-ground synchrony across local temperature variation and plant communities (**Table S2**). While there were no significant differences in synchrony between graminoid-dominated and shrub-dominated communities, we found that the proportion of total root biomass at the time of peak above-ground greenness was 47% higher for graminoid relative to mixed-species communities (-5.49 g cm^{-3}, CI: -9.51 to -1.42).
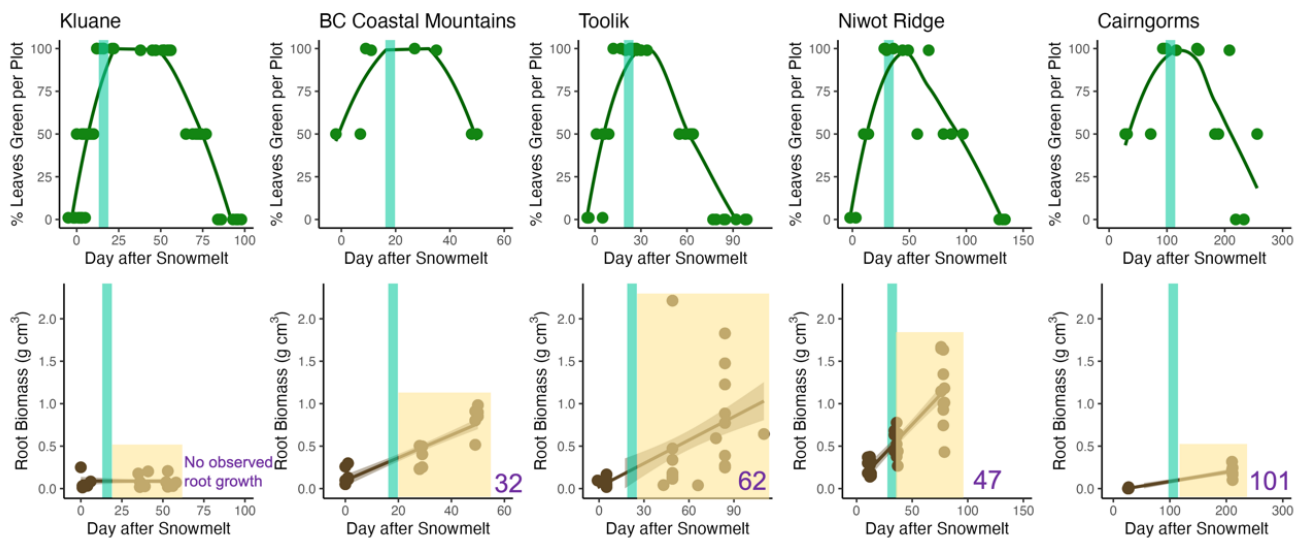
x = Number of days of observed root growth after the date of peak aboveground growth

Figure 2. Root growth continues after above-ground plant tissues begin to senesce across all but one site. Top panel represents phenocam-derived greening curves for each site, with each green point representing the date after 100% snowmelt per plot that a recorded phenophase occurred (bud burst, 50% green leaves, 100% green leaves, first yellow leaf, 50% yellow leaves, and 100% yellow leaves). Brown points in the bottom panel represent the root biomass per g cm^{-3} of dry bulk soil density averaged across each in-growth core corresponding to their extraction from the experiment and the timing of that extraction in relation to the date of 100% snowmelt per plot. Teal vertical lines represent the site-averaged dates of peak aboveground growth, or the mean 'day after snowmelt' that plots reached 100% green leaves. Yellow coloured backgrounds represent senescence (yellow). Sites are ordered here by time taken to achieve full green-up, from fastest (Kluane) to slowest (Cairngorms). Purple numeric labels on the bottom panel indicate the number of days of observed root growth beyond the date of peak aboveground productivity, excluded for Kluane because there was no observed biomass

473   increase over time at this site. Yellow shading represents the length and magnitude of root

474   growth after above-ground growth peaks.

475

476   Root biomass varied significantly by community type across the sites (**Fig. 3**, **Fig. S2a**, **Table**

477   **S2**). We found that in-growth cores from graminoid-dominated communities had 41% higher

478   root biomass than shrub-dominated communities (categorical difference of 0.12 g cm^{-3}, CI:

479   0.03 to 0.24) and 36% higher biomass than mixed-species communities (categorical difference

480   of 0.14 g cm^{-3}, CI: -0.02 to -0.01). Likewise, daily root growth rates (i.e., rate of daily root

481   growth as calculated between first and last core harvest; **Table S2b**; see **Equation 2)** were

482   faster in graminoid, relative to mixed and shrub dominated plant communities (**Fig. 3**, **Fig. S4,**

483   **Table S2**), with in-growth cores installed in graminoid-dominated plots exhibiting daily root

484   growth rates 51% faster than shrub-dominated communities (shrub slope: -0.01 g cm^{-3} per day,

485   CI: -0.01 to -0.002), and 61% faster than mixed-species communities (mixed slope: -0.01 g cm^{-}

486   ^{3} per day, CI: -0.01 to -0.004).

487
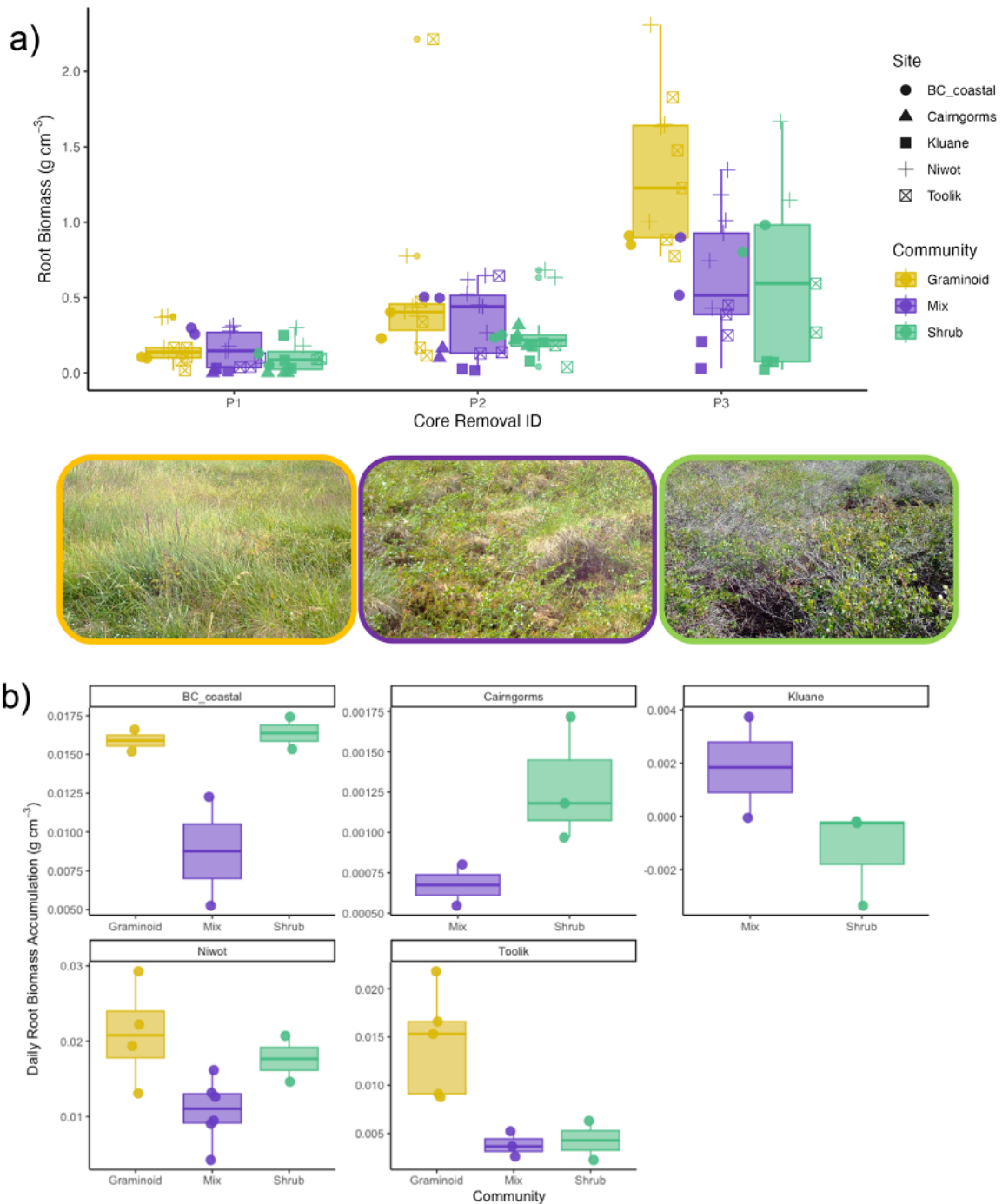
Figure 3. (a) Root biomass accumulation was greater for graminoid-dominated relative to shrub-dominated plots. Error bars represent the distributions of the root biomass per bulk density (g cm^{-3}) for each stage of removal (P1, P2 or P3) across the three community types: graminoid-dominated, mixture of graminoid and shrub, shrub-dominated. Points represent the root biomass per g cm^{-3} of dry bulk soil density averaged across each in-growth core. Photos are select screenshots from 9th July 2021 across three Toolik Lake plots representing the corresponding community types (Image Credits: Ruby An). (b) Root growth rates were generally faster at the graminoid-dominated plots than the shrub-dominated or mixed-species

497 plots. Error bars represent the distributions of the daily root biomass accumulation (g cm^{-3})

498 across the summer across the three community types. Points represent the daily root biomass

499 accumulation per g cm^{-3} of dry bulk soil density averaged across each in-growth core cluster.

500

501 Contrary to our predictions, root biomass did not vary across microclimate (**Fig. 4, Table S2a**).

502 The difference in root biomass per bulk dry soil density between the coldest and warmest

503 microclimate groupings was -0.001 g cm^{-3} (-0.015 to 0.014). Similarly, daily root growth rates

504 (i.e., daily rate of root growth as calculated between first and last core harvest) across the
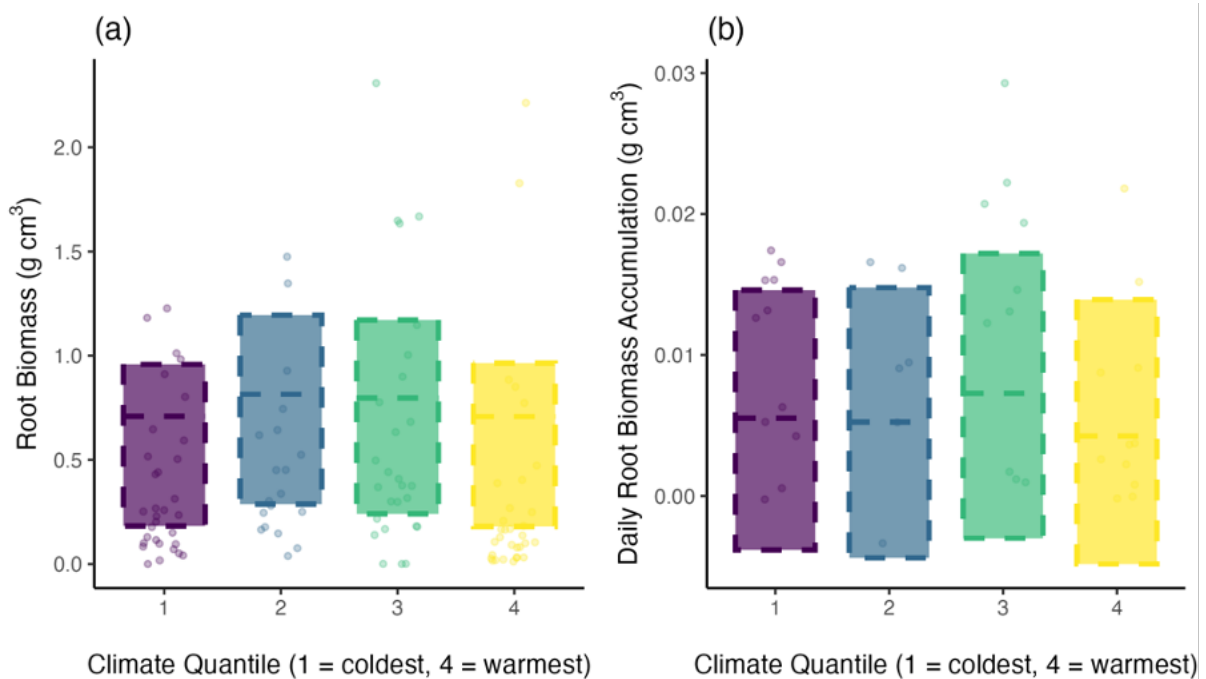
505 growing season were not significantly different between across surface temperature quantiles

506 (**Table S2b**). For example, the difference in root growth rate per day between the coldest and

507 warming quantile groupings was -0.0012 g cm^{-3} day^{-1} (-0.0061 to 0.0035). For all model

508 designs, the top 5cm only model results revealed the same trends (**Table S3**).

509

510

511

512 **Figure 4.** Root biomass allocation and root growth rates did not correspond with local surface

513 temperature. Error bars in (a) represent the modelled distributions (Table S2a) of the root

514 biomass / bulk density (g cm^{-3}) for the final stage of removal (P3), plotted across summer

515 surface temperature microclimate quantile groups. Error bars in (b) represent the modelled

516 distributions (Table S2b) of the daily root growth rates between P3 and P1, plotted across

517 summer surface temperature microclimate quantile groups. Points represent the root biomass

518 per g cm^{-3} of dry bulk soil density averaged across each in-growth core.

18

Discussion

Synthesis

As predicted, we found that above-ground leaf phenology and below-ground root phenology was asynchronous across all sites, with root growth continuing long after the timing above-ground peak productivity **(Fig. 2)**. At some sites there was evidence that the below-ground growing season extended beyond the point of 50% above-ground leaf senescence, although without continuous core removals later in the season it was not possible to determine the time of root growth cessation **(Fig. 2)**. Our findings from five sites from the Western Arctic, North American and Scottish alpine tundra correspond with studies from Arctic Sweden and Western Greenland (Blume-Werry et al., 2016; Radville et al., 2016; Sullivan et al., 2007). Taken together, we now have compelling evidence that above- and below- ground tundra phenology is asynchronous and that the below-ground growing season can extend 50% longer than the above ground growing season (Blume-Werry et al., 2016; Radville et al., 2016; Sullivan et al., 2007). Importantly in this cross-site study, we found that vegetation community composition, rather than microclimate, had the greatest influence on root biomass accumulation and root growth rates. We found that root biomass was greater and root growth rates faster in graminoid-dominated relative to shrub-dominated plots (**Fig. 3**). Additionally, we observed a distinct peak in root growth in graminoid-dominated plots, usually taking place towards the end of the above-ground growing season, while root biomass accumulated more linearly over time in the mixed-species and shrub-dominated plots **(Fig. 3; Fig. S4)**. Contrary to our hypotheses, we found no correspondence between microclimate and root biomass accumulation, daily root growth rates or above- versus below-ground phenological asynchrony **(Fig. 4).** This analysis therefore highlights that plant community types rather than microclimates may be the most important influence on root productivity and the timing of root growth.

Root biomass was higher - and growth rates faster - in graminoid dominated plots

We found that root biomass was greater and daily root growth rates were faster in the graminoid-dominated plots than shrub-dominated or mixed-species plots **(Fig. 3**; **Table S3a)**. Many studies highlight different root growth strategies between and within plant functional types, often noting that graminoid species will forage root later in the growing season, and in deeper soils, in order to access nutrients available at the permafrost thaw front (Blume-Werry et al., 2019; Hewitt et al., 2019; Keuper et al., 2017; McKane et al., 2002; Pedersen et al., 2020; Salmon et al., 2018; Schwieger et al., 2018; Sullivan et al., 2007). Annual root turnover by

553   sedge communities already contributes significantly to net primary productivity (NPP) in the
554   tundra (Iversen et al., 2015; Sloan, 2011; Sloan et al., 2013). In areas where conditions are
555   projected to become more mesic and provide optimal habitat to support graminoid expansion
556   (Andresen & Lougheed, 2021; Heijmans et al., 2022), NPP may therefore increase. However,
557   in areas where woody shrubs outcompete other plant species (Mekonnen et al., 2018), root
558   biomass may be reduced, particularly at depths close to the active layer thaw front. Different
559   root biomass and growth characteristics are likely, therefore, to influence local and regional
560   carbon flux dynamics in areas where tundra vegetation composition is predicted to reshuffle,
561   potentially bringing carbon stores towards the surface with increasing shrub cover.

562

563   We found that daily root growth rates were significantly faster in graminoid-dominated
564   communities than mixed-species or shrub-dominated communities **(Fig. 3**; **Table S2b),** which
565   was particularly defined by a visible graminoid growth peak towards the end of the growing
566   season in comparison to a more linear growth rate in the other plots **(Fig. 3**; **Table S2b)**. This
567   rapid increase in biomass in late summer may reflect enhanced uptake of nutrients by graminoid
568   roots towards the end of the growing season when this abundant nutrient source is made
569   available by thaw (Hewitt et al., 2019; Keuper et al., 2017; Pedersen et al., 2020; Wang et al.,
570   2017). If this ability to harness nutrients late-season is unique to deep-rooting graminoid
571   species, these results potentially challenge the assumption that shrubs have a competitive
572   advantage in warming tundra landscapes (Mekonnen et al., 2018), or at least emphasise that
573   rooting strategies differ greatly across plant communities. Furthermore, in areas where we are
574   seeing an advancement in both the green-up and the onset of senescence within the
575   aboveground growing season (Gallois et al., *in prep*), extensions of the belowground growing
576   season could extend the length of the total growing season and increase the above-ground
577   below-ground asynchrony.

578

579   ***Root productivity and phenology did not correspond to spatial variation in surface***
580   ***temperature***
581   Across these five tundra sites representing variation in topography and landscape
582   heterogeneity, root growth rates and root biomass did not vary consistently across surface
583   temperature ranges within sites **(Fig. 4, Table S2)**. Previous research presents contrasting
584   evidence on the influence of microclimate on root productivity and phenology in tundra
585   ecosystems. For example, field studies using experimentally warmed plots often indicate that
586   the timing of the start of the below-ground growing season, and the length of this growing

season, are generally unaffected by increased temperatures (Ma et al., 2022; Radville et al., 2018), however, warming may increase total root biomass (Collins 2024, unpublished data; Wang et al., 2017). Likewise, experimental snowmelt removal indicates that while advanced snowmelt often leads to an advanced above-ground growing season, the timing of root phenology is largely unaltered (Blume-Werry et al., 2017; Möhl et al., 2022). In contrast, Liu *et al* (2021) found that the below-ground growing season at a tundra site lengthened by approximately two days for each additional 1°C of warming. The timing of phenophases above-ground appears to be driven jointly by variation in snowmelt timing and surface microclimatic conditions (Assmann et al., 2019; Jerome et al., 2021; Kelsey et al., 2021). Taken together, root phenology does not appear to have the same degree of sensitivity to microclimate indicates the potential for further above- versus below-ground asynchrony under climate warming scenarios.

These five study sites varied in their permafrost status and depth to permafrost with Toolik Lake being underlain by ice-rich permafrost, alpine sites being underlain by discontinuous mountain permafrost, and the more southerly Cairngorms site being underlain by bedrock. There is evidence to suggest that root growth is enhanced where permafrost thaw is deeper (Hewitt et al., 2019; Keuper et al., 2017; Pedersen et al., 2020). Permafrost active layers are highly spatially heterogeneous, and typically deeper in correspondence with warmer air temperatures (Biskaborn et al., 2019; Yi et al., 2018). In alpine soils, root growth is strongly limited by soil temperature due to the cessation of cell elongation and differentiation below 0.8 to 1.2°C (Nagelmüller et al., 2017; Sebastian et al., 2016). The average summer soil temperature at 6 cm depth was over 5°C across all sites (**Table S1,** not including plots where logger readings were corrupted), so it is likely that the roots in this study were not subject to soil temperatures below their thermal tolerance in summer. It is also possible that above this thermal threshold of 0.8 to 1.2°C, temperature no longer controls root growth patterns. Tundra roots may be more strongly influenced by alternative abiotic conditions such as the depth of available soil nutrients or water. The site with the warmest July-August surface temperatures (Toolik Lake; **Table S1**) had the greatest end-of-season root biomass, while the site with the coldest summer surface temperatures (Kluane; **Table S1**) had the lowest end-of-season root biomass. While both the timing of core extractions and overall levels of biomass varied by site, it is possible that on a macro-scale, if not a micro-scale, warmer summer conditions may prompt greater root growth.

Above- and below-ground phenology are not synchronised

As predicted, above- and below-ground root phenology was asynchronous across almost all sites, with root growth continuing up to 74% after the above-ground peak in leaf phenology **(Fig. 3)**. However, we found no correspondence between microclimate and phenological synchrony (**Table S2c**). These findings directly support observations that the below-ground growing season in tundra ecosystems can significantly extend beyond the above-ground growing season, in accordance with studies in Arctic Sweden and Western Greenland (Blume-Werry, 2021; Blume-Werry et al., 2016; Liu et al., 2021; Radville et al., 2016; Sullivan et al., 2007). Adding five additional sites to existing studies, our results provide a cross-biome perspective that is critical for improved understanding of tundra carbon cycling. Plant phenology is intrinsically tied to carbon cycling with tundra ecosystems - with increased vegetation productivity increasing uptake of atmospheric carbon, and longer growing seasons triggering increased respiration towards the end of the summer (Bruhwiler et al., 2021; Ueyama et al., 2013). The drivers of above- versus below-ground phenology in the tundra may be decoupled, potentially as a function of internal nutrient and hormone allocation timings within plants (Abramoff & Finzi, 2015), or via the varying physiological relevance of above-ground conditions such as air temperature versus below-ground conditions such as thaw depth (Liu et al., 2021). In areas where the aboveground growing season advances, and the belowground growing season extends long after peak leaf productivity, the total growing season incorporating both above-ground and below-ground plant components is therefore lengthened and elements of plant productivity functionally decoupled.

Scope for future research

While these results showcase clear asynchrony in root productivity and phenology between tundra vegetation community types, key questions remain. Firstly, we were only able to capture summer growing season dynamics in this study and could therefore not quantify root growth throughout the entirety of the potential growing season as we were not able to quantify the cessation of root growth. However, there is evidence that root growth may be possible outside of the snow-free period where photosynthesis and growth are constrained by snow cover and light (Blume-Werry et al., 2017; Riley et al., 2021). A priority for future research will be to investigate how much root growth occurs outside of the snow-free season window, both before spring snowmelt and after autumn snow-return. Our analyses revealed evidence of late-season root-growth 'peaks' in graminoid dominated plots, which may at some sites (such as Toolik) be exacerbated by permafrost thaw dynamics. Analysis of both thaw depth and root growth

over the course of one growing season using a fine temporal resolution could help identify whether graminoid root growth and rooting depth closely track the timing of active layer thaw (see: Blume-Werry et al., 2019; Hewitt et al., 2019; Keuper et al., 2017; Shaver & Billings, 1975), and pinpoint the extent to which these phenomena track aboveground phenology. Future analysis could use the significantly varying below-ground biomass and growth rate data alongside projections of future vegetation range shifts to scale up projections of both carbon uptake and carbon respiration from root systems in tundra ecosystems. Finally, the methods we used for this study could easily be extended over the course of time to analyse the difference between above- and below-ground phenology and root yield in warmer and colder years. Critically, extending these analyses across multiple years (and a greater number of sites) could further refine our understanding of how above- versus below-ground asynchrony is changing spatiotemporally.

Conclusion

The tundra biome is undergoing a rapid shift in vegetation towards more shrub and graminoid dominated plant communities as the climate warms (Berner & Goetz, 2022; Bhatt et al., 2013; Elmendorf et al., 2012; Forbes et al., 2010, 2010; Myers-Smith et al., 2011, 2020). We found that below-ground root growth continues late into the tundra growing season **(Fig. 2)**, offset by an average of 56 days from the peak of plant growth above-ground. Graminoid-dominated communities had a much higher root biomass density than shrub-dominated and mix-species communities **(Fig. 3**; **Table S2a)**, and also exhibited a clear late-season root growth 'pulse' in comparison to more linear growth trends across other community types **(Fig. 3**; **Fig. S4**; **Table S2b)**. Contrary to our expectations, we found no clear correspondence between root productivity or phenology and local surface temperature variation **(Fig. 4**; **Table S2)**, suggesting that indirect effects of warming on vegetation change might be a more important driver than the direct effects of warming on below-ground root growth and dynamics. Taken together, this study highlights that changes in the vegetation community type could influence root biomass and root growth rates in Arctic and alpine tundra with important implications for carbon cycling (Jones et al., 2009; Sokol & Bradford, 2019).

The drivers of root growth and phenology are critically understudied, and the importance of roots in tundra carbon cycling is commonly oversimplified in Earth systems models (Smithwick et al., 2014; Warren et al., 2015; Blume-Werry et al., 2023). Roots constitute

688   approximately 80% of the total biomass within the tundra ecosystem (Mokany et al., 2006) and

689   provide both an efficient mechanism for stable sequestration of atmospheric carbon (Jones et

690   al., 2009; Sokol & Bradford, 2019) and a substantial source of carbon to be decomposed and

691   respired back into the atmosphere (Sullivan et al., 2007; Zona et al., 2022). Root dynamics

692   underpin plant productivity and carbon sequestration in one of the most rapidly changing

693   biomes on the planet, and therefore incorporating these processes into global climate models

694   will critically enhance our ability to predict carbon fluxes. The results from this study reveal a

695   clear pathway toward modelling these changes – by using above-ground community

696   composition to estimate below-ground productivity and phenology.

Reference List

Abramoff, R. Z., & Finzi, A. C. (2015). Are above- and below-ground phenology in sync? *New Phytologist*, *205*(3), 1054–1061. https://doi.org/10.1111/nph.13111

Andresen, C. G., & Lougheed, V. L. (2021). Arctic aquatic graminoid tundra responses to nutrient availability. *Biogeosciences*, *18*(8), 2649–2662. https://doi.org/10.5194/bg-18-2649-2021

Assmann, J. J., Myers-Smith, I. H., Phillimore, A. B., Bjorkman, A. D., Ennos, R. E., Prevéy, J. S., Henry, G. H., Schmidt, N. M., & Hollister, R. D. (2019). Local snow melt and temperature—But not regional sea ice—Explain variation in spring phenology in coastal Arctic tundra. *Global Change Biology*, *25*(7), 2258–2274.

Berner, L. T., & Goetz, S. J. (2022). Satellite observations document trends consistent with a boreal forest biome shift. *Global Change Biology*, *28*(10), 3275–3292. https://doi.org/10.1111/gcb.16121

Bhatt, U. S., Walker, D. A., Raynolds, M. K., Bieniek, P. A., Epstein, H. E., Comiso, J. C., Pinzon, J. E., Tucker, C. J., & Polyakov, I. V. (2013). Recent Declines in Warming and Vegetation Greening Trends over Pan-Arctic Tundra. *Remote Sensing*, *5*(9), Article 9. https://doi.org/10.3390/rs5094229

Biskaborn, B. K., Smith, S. L., Noetzli, J., Matthes, H., Vieira, G., Streletskiy, D. A., Schoeneich, P., Romanovsky, V. E., Lewkowicz, A. G., Abramov, A., Allard, M., Boike, J., Cable, W. L., Christiansen, H. H., Delaloye, R., Diekmann, B., Drozdov, D., Etzelmüller, B., Grosse, G., … Lantuit, H. (2019). Permafrost is warming at a global scale. *Nature Communications*, *10*(1), Article 1. https://doi.org/10.1038/s41467-018-08240-4

Bjorkman, A. D., Elmendorf, S. C., Beamish, A. L., Vellend, M., & Henry, G. H. R. (2015). Contrasting effects of warming and increased snowfall on Arctic tundra plant phenology over the past two decades. *Global Change Biology*, *21*(12), 4651–4661. https://doi.org/10.1111/gcb.13051

Bjorkman, A. D., García Criado, M., Myers-Smith, I. H., Ravolainen, V., Jónsdóttir, I. S., Westergaard, K. B., Lawler, J. P., Aronsson, M., Bennett, B., Gardfjell, H., Heiðmarsson, S., Stewart, L., & Normand, S. (2020). Status and trends in Arctic vegetation: Evidence from experimental warming and long-term monitoring. *Ambio*, *49*(3), 678–692. https://doi.org/10.1007/s13280-019-01161-6

Blume-Werry, G. (2021). The belowground growing season. *Nature Climate Change*, 1–2. https://doi.org/10.1038/s41558-021-01243-y

Blume-Werry, G., Jansson, R., & Milbau, A. (2017). Root phenology unresponsive to earlier snowmelt despite advanced above-ground phenology in two subarctic plant communities. *Functional Ecology*, *31*(7), 1493–1502. https://doi.org/10.1111/1365-2435.12853

Blume-Werry, G., Milbau, A., Teuber, L. M., Johansson, M., & Dorrepaal, E. (2019). Dwelling in the deep – strongly increased root growth and rooting depth enhance plant interactions with thawing permafrost soil. *New Phytologist*, *223*(3), 1328–1339. https://doi.org/10.1111/nph.15903

Blume-Werry, G., Wilson, S. D., Kreyling, J., & Milbau, A. (2016). The hidden season: Growing season is 50% longer below than above ground along an arctic elevation gradient. *New Phytologist*, *209*(3), 978–986.

Bruhwiler, L., Parmentier, F.-J. W., Crill, P., Leonard, M., & Palmer, P. I. (2021). The Arctic Carbon Cycle and Its Response to Changing Climate. *Current Climate Change Reports*, *7*(1), 14–34. https://doi.org/10.1007/s40641-020-00169-5

Bürkner, P.-C. (2017). brms: An R package for Bayesian multilevel models using Stan. *Journal of Statistical Software*, *80*(1), 1–28.

de Kroon, H., Hendriks, M., van Ruijven, J., Ravenek, J., Padilla, F. M., Jongejans, E., Visser, E. J. W., & Mommer, L. (2012). Root responses to nutrients and soil biota: Drivers of species coexistence and ecosystem productivity. *Journal of Ecology*, *100*(1), 6–15. https://doi.org/10.1111/j.1365-2745.2011.01906.x

Elmendorf, S. C., Henry, G. H., Hollister, R. D., Björk, R. G., Boulanger-Lapointe, N., Cooper, E. J., Cornelissen, J. H., Day, T. A., Dorrepaal, E., & Elumeeva, T. G. (2012). Plot-scale evidence of tundra vegetation change and links to recent summer warming. *Nature Climate Change*, *2*(6), 453–457.

Forbes, B. C., Fauria, M. M., & Zetterberg, P. (2010). Russian Arctic warming and 'greening' are closely tracked by tundra shrub willows. *Global Change Biology*, *16*(5), 1542–1554. https://doi.org/10.1111/j.1365-2486.2009.02047.x

Freschet, G. T., Pagès, L., Iversen, C. M., Comas, L. H., Rewald, B., Roumet, C., Klimešová, J., Zadworny, M., Poorter, H., Postma, J. A., Adams, T. S., Bagniewska-Zadworna, A., Bengough, A. G., Blancaflor, E. B., Brunner, I., Cornelissen, J. H. C., Garnier, E., Gessler, A., Hobbie, S. E., … McCormack, M. L. (2021). A starting guide to root ecology: Strengthening ecological

concepts and standardising root classification, sampling, processing and trait measurements. *New Phytologist*, *232*(3), 973–1122. https://doi.org/10.1111/nph.17572

Gallois, E.C, Myers-Smith, I.H., Bjorkman, A.D., Elmendorf, S.E., Anderson, M., de Jong G, Grenier, M. (in prep). *Tundra peak productivity is earlier in warmer summers and warmer microclimates, while growing season lengths remain constant.*

García Criado, M., Myers-Smith, I. H., Bjorkman, A. D., Lehmann, C. E. R., & Stevens, N. (2020). Woody plant encroachment intensifies under climate change across tundra and savanna biomes. *Global Ecology and Biogeography*, *29*(5), 925–943. https://doi.org/10.1111/geb.13072

Guderle, M., Bachmann, D., Milcu, A., Gockele, A., Bechmann, M., Fischer, C., Roscher, C., Landais, D., Ravel, O., Devidal, S., Roy, J., Gessler, A., Buchmann, N., Weigelt, A., & Hildebrandt, A. (2018). Dynamic niche partitioning in root water uptake facilitates efficient water use in more diverse grassland plant communities. *Functional Ecology*, *32*(1), 214–227. https://doi.org/10.1111/1365-2435.12948

Heijmans, M. M. P. D., Magnússon, R. Í., Lara, M. J., Frost, G. V., Myers-Smith, I. H., van Huissteden, J., Jorgenson, M. T., Fedorov, A. N., Epstein, H. E., Lawrence, D. M., & Limpens, J. (2022). Tundra vegetation change and impacts on permafrost. *Nature Reviews Earth & Environment*, *3*(1), Article 1. https://doi.org/10.1038/s43017-021-00233-0

Hewitt, R. E., Taylor, D. L., Genet, H., McGuire, A. D., & Mack, M. C. (2019). Below-ground plant traits influence tundra plant acquisition of newly thawed permafrost nitrogen. *Journal of Ecology*, *107*(2), 950–962. https://doi.org/10.1111/1365-2745.13062

Høye, T. T., Post, E., Meltofte, H., Schmidt, N. M., & Forchhammer, M. C. (2007). Rapid advancement of spring in the High Arctic. *Current Biology*, *17*(12), R449–R451. https://doi.org/10.1016/j.cub.2007.04.047

Iversen, C. M., Sloan, V. L., Sullivan, P. F., Euskirchen, E. S., McGuire, A. D., Norby, R. J., Walker, A. P., Warren, J. M., & Wullschleger, S. D. (2015). The unseen iceberg: Plant roots in arctic tundra. *New Phytologist*, *205*(1), 34–58. https://doi.org/10.1111/nph.13003

798   Jones, D. L., Nguyen, C., & Finlay, R. D. (2009). Carbon flow in the rhizosphere:
799   Carbon trading at the soil–root interface. *Plant and Soil*, *321*(1), 5–33.
800   https://doi.org/10.1007/s11104-009-9925-0

801   Keuper, F., Dorrepaal, E., van Bodegom, P. M., van Logtestijn, R., Venhuizen, G., van
802   Hal, J., & Aerts, R. (2017). Experimentally increased nutrient availability at the
803   permafrost thaw front selectively enhances biomass production of deep-rooting
804   subarctic peatland species. *Global Change Biology*, *23*(10), 4257–4266.
805   https://doi.org/10.1111/gcb.13804

806   Liu, H., Wang, H., Li, N., Shao, J., Zhou, X., van Groenigen, K. J., & Thakur, M. P.
807   (2021). Phenological mismatches between above- and belowground plant
808   responses to climate warming. *Nature Climate Change*, 1–6.
809   https://doi.org/10.1038/s41558-021-01244-x

810   Ma, H., Mo, L., Crowther, T. W., Maynard, D. S., van den Hoogen, J., Stocker, B. D.,
811   Terrer, C., & Zohner, C. M. (2021). The global distribution and environmental
812   drivers of aboveground versus belowground plant biomass. *Nature Ecology &*
813   *Evolution*, *5*(8), Article 8. https://doi.org/10.1038/s41559-021-01485-1

814   Ma, T., Parker, T., Fetcher, N., Unger, S. L., Gewirtzman, J., Moody, M. L., & Tang,
815   J. (2022). Leaf and root phenology and biomass of *Eriophorum vaginatum* in
816   response to warming in the Arctic. *Journal of Plant Ecology*, *15*(5), 1091–1105.
817   https://doi.org/10.1093/jpe/rtac010

818   Martin, A. C., Jeffers, E. S., Petrokofsky, G., Myers-Smith, I., & Macias-Fauria, M.
819   (2017). Shrub growth and expansion in the Arctic tundra: An assessment of
820   controlling factors using an evidence-based approach. *Environmental Research*
821   *Letters*, *12*(8), 085007. https://doi.org/10.1088/1748-9326/aa7989

822   McKane, R. B., Johnson, L. C., Shaver, G. R., Nadelhoffer, K. J., Rastetter, E. B., Fry,
823   B., Giblin, A. E., Kielland, K., Kwiatkowski, B. L., Laundre, J. A., & Murray,
824   G. (2002). Resource-based niches provide a basis for plant species diversity and
825   dominance in arctic tundra. *Nature*, *415*(6867), Article 6867.
826   https://doi.org/10.1038/415068a

827   Mekonnen, Z. A., Riley, W. J., & Grant, R. F. (2018). Accelerated Nutrient Cycling
828   and Increased Light Competition Will Lead to 21st Century Shrub Expansion
829   in North American Arctic Tundra. *Journal of Geophysical Research:*
830   *Biogeosciences*, *123*(5), 1683–1701. https://doi.org/10.1029/2017JG004319

Möhl, P., von Büren, R. S., & Hiltbrunner, E. (2022). Growth of alpine grassland will start and stop earlier under climate warming. *Nature Communications*, *13*(1), Article 1. https://doi.org/10.1038/s41467-022-35194-5

Mokany, K., Raison, R. J., & Prokushkin, A. S. (2006). Critical analysis of root: Shoot ratios in terrestrial biomes. *Global Change Biology*, *12*(1), 84–96. https://doi.org/10.1111/j.1365-2486.2005.001043.x

Myers-Smith, I. H., Forbes, B. C., Wilmking, M., Hallinger, M., Lantz, T., Blok, D., Tape, K. D., Macias-Fauria, M., Sass-Klaassen, U., & Lévesque, E. (2011). Shrub expansion in tundra ecosystems: Dynamics, impacts and research priorities. *Environmental Research Letters*, *6*(4), 045509.

Myers-Smith, I. H., Kerby, J. T., Phoenix, G. K., Bjerke, J. W., Epstein, H. E., Assmann, J. J., John, C., Andreu-Hayles, L., Angers-Blondin, S., Beck, P. S. A., Berner, L. T., Bhatt, U. S., Bjorkman, A. D., Blok, D., Bryn, A., Christiansen, C. T., Cornelissen, J. H. C., Cunliffe, A. M., Elmendorf, S. C., … Wipf, S. (2020). Complexity revealed in the greening of the Arctic. *Nature Climate Change*, *10*(2), Article 2. https://doi.org/10.1038/s41558-019-0688-1

Nagelmüller, S., Hiltbrunner, E., & Körner, C. (2017). Low temperature limits for root growth in alpine species are set by cell differentiation. *AoB PLANTS*, *9*(6), plx054. https://doi.org/10.1093/aobpla/plx054

Naito, A. T., & Cairns, D. M. (2011). Patterns and processes of global shrub expansion. *Progress in Physical Geography: Earth and Environment*, *35*(4), 423–442. https://doi.org/10.1177/0309133311403538

Niittynen, P., Heikkinen, R. K., & Luoto, M. (2020). Decreasing snow cover alters functional composition and diversity of Arctic tundra. *Proceedings of the National Academy of Sciences*, *117*(35), 21480–21487. https://doi.org/10.1073/pnas.2001254117

Panchen, Z. A., & Gorelick, R. (2015). Flowering and fruiting responses to climate change of two Arctic plant species, purple saxifrage (Saxifraga oppositifolia) and mountain avens (Dryas integrifolia). *Arctic Science*, *1*(2), 45–58. https://doi.org/10.1139/as-2015-0016

Panchen, Z. A., & Gorelick, R. (2017). Prediction of Arctic plant phenological sensitivity to climate change from historical records. *Ecology and Evolution*, *7*(5), 1325–1338. https://doi.org/10.1002/ece3.2702

864 Pedersen, E. P., Elberling, B., & Michelsen, A. (2020). Foraging deeply: Depth-specific
865   plant nitrogen uptake in response to climate-induced N-release and permafrost
866   thaw in the High Arctic. *Global Change Biology*, *26*(11), 6523–6536.
867   https://doi.org/10.1111/gcb.15306

868 Prevéy, J. S., Rixen, C., Rüger, N., Høye, T. T., Bjorkman, A. D., Myers-Smith, I. H.,
869   Elmendorf, S. C., Ashton, I. W., Cannone, N., Chisholm, C. L., Clark, K.,
870   Cooper, E. J., Elberling, B., Fosaa, A. M., Henry, G. H. R., Hollister, R. D.,
871   Jónsdóttir, I. S., Klanderud, K., Kopp, C. W., … Wipf, S. (2019). Warming
872   shortens flowering seasons of tundra plant communities. *Nature Ecology &*
873   *Evolution*, *3*(1), Article 1. https://doi.org/10.1038/s41559-018-0745-6

874 Prevéy, J., Vellend, M., Rüger, N., Hollister, R. D., Bjorkman, A. D., Myers-Smith, I.
875   H., Elmendorf, S. C., Clark, K., Cooper, E. J., Elberling, B., Fosaa, A. M.,
876   Henry, G. H. R., Høye, T. T., Jónsdóttir, I. S., Klanderud, K., Lévesque, E.,
877   Mauritz, M., Molau, U., Natali, S. M., … Rixen, C. (2017). Greater temperature
878   sensitivity of plant phenology at colder sites: Implications for convergence
879   across northern latitudes. *Global Change Biology*, *23*(7), 2660–2671.
880   https://doi.org/10.1111/gcb.13619

881 Radville, L., Bauerle, T. L., Comas, L. H., Marchetto, K. A., Lakso, A. N., Smart, D.
882   R., Dunst, R. M., & Eissenstat, D. M. (2016). Limited linkages of aboveground
883   and belowground phenology: A study in grape. *American Journal of Botany*,
884   *103*(11), 1897–1911. https://doi.org/10.3732/ajb.1600212

885 Radville, L., Post, E., & Eissenstat, D. M. (2018). On the sensitivity of root and leaf
886   phenology to warming in the Arctic. *Arctic, Antarctic, and Alpine Research*,
887   *50*(1), S100020. https://doi.org/10.1080/15230430.2017.1414457

888 Riley, W. J., Mekonnen, Z. A., Tang, J., Zhu, Q., Bouskill, N. J., & Grant, R. F. (2021).
889   Non-growing season plant nutrient uptake controls Arctic tundra vegetation
890   composition under future climate. *Environmental Research Letters*, *16*(7),
891   074047. https://doi.org/10.1088/1748-9326/ac0e63

892 Salmon, V. G., Schädel, C., Bracho, R., Pegoraro, E., Celis, G., Mauritz, M., Mack, M.
893   C., & Schuur, E. A. G. (2018). Adding Depth to Our Understanding of Nitrogen
894   Dynamics in Permafrost Soils. *Journal of Geophysical Research:*
895   *Biogeosciences*, *123*(8), 2497–2512. https://doi.org/10.1029/2018JG004518

Schenk, H. J., & Jackson, R. B. (2002). The Global Biogeography of Roots. *Ecological Monographs*, *72*(3), 311–328. https://doi.org/10.1890/0012-9615(2002)072[0311:TGBOR]2.0.CO;2

Schwieger, S., Kreyling, J., Milbau, A., & Blume-Werry, G. (2018). Autumnal warming does not change root phenology in two contrasting vegetation types of subarctic tundra. *Plant and Soil*, *424*(1), 145–156. https://doi.org/10.1007/s11104-017-3343-5

Sebastian, N., Erika, H., & Christian, K. (2016). Critically low soil temperatures for root growth and root morphology in three alpine plant species. *Alpine Botany*, *126*(1), 11–21. https://doi.org/10.1007/s00035-015-0153-3

Shaver, G. R., & Billings, W. D. (1975). Root Production and Root Turnover in a Wet Tundra Ecosystem, Barrow, Alaska. *Ecology*, *56*(2), 401–409. https://doi.org/10.2307/1934970

Sloan, V. L. (2011). *Plant roots in Arctic ecosystems: Stocks and dynamics, and their coupling to above-ground parameters* [Ph.D., The University of Sheffield]. https://ethos.bl.uk/OrderDetails.do?uin=uk.bl.ethos.544159

Sloan, V. L., Fletcher, B. J., Press, M. C., Williams, M., & Phoenix, G. K. (2013). Leaf and fine root carbon stocks and turnover are coupled across Arctic ecosystems. *Global Change Biology*, *19*(12), 3668–3676. https://doi.org/10.1111/gcb.12322

Smithwick, E. A. H., Lucash, M. S., McCormack, M. L., & Sivandran, G. (2014). Improving the representation of roots in terrestrial models. *Ecological Modelling*, *291*, 193–204. https://doi.org/10.1016/j.ecolmodel.2014.07.023

Snow, Water, Ice and Permafrost in the Arctic (SWIPA) 2017 | AMAP. (n.d.). Retrieved 8 August 2023, from https://www.amap.no/documents/doc/snow-water-ice-and-permafrost-in-the-arctic-swipa-2017/1610

Sokol, N. W., & Bradford, M. A. (2019). Microbial formation of stable soil carbon is more efficient from belowground than aboveground input. *Nature Geoscience*, *12*(1), Article 1. https://doi.org/10.1038/s41561-018-0258-6

Sullivan, P. F., Sommerkorn, M., Rueth, H. M., Nadelhoffer, K. J., Shaver, G. R., & Welker, J. M. (2007). Climate and species affect fine root production with long-term fertilization in acidic tussock tundra near Toolik Lake, Alaska. *Oecologia*, *153*(3), 643–652.

Tape, K. E. N., Sturm, M., & Racine, C. (2006). The evidence for shrub expansion in Northern Alaska and the Pan-Arctic. *Global Change Biology*, *12*(4), 686–702.

Team, R. C. (2013). *R: A language and environment for statistical computing*.

Ueyama, M., Iwata, H., Harazono, Y., Euskirchen, E. S., Oechel, W. C., & Zona, D. (2013). Growing season and spatial variations of carbon fluxes of Arctic and boreal ecosystems in Alaska (USA). *Ecological Applications*, *23*(8), 1798–1816. https://doi.org/10.1890/11-0875.1

Warren, J. M., Hanson, P. J., Iversen, C. M., Kumar, J., Walker, A. P., & Wullschleger, S. D. (2015). Root structural and functional dynamics in terrestrial biosphere models – evaluation and recommendations. *New Phytologist*, *205*(1), 59–78. https://doi.org/10.1111/nph.13034

Wookey, P. A., Parsons, A. N., Welker, J. M., Potter, J. A., Callaghan, T. V., Lee, J. A., & Press, M. C. (1993). Comparative Responses of Phenology and Reproductive Development to Simulated Environmental Change in Sub-Arctic and High Arctic Plants. *Oikos*, *67*(3), 490–502. https://doi.org/10.2307/3545361

Yi, Y., Kimball, J. S., Chen, R. H., Moghaddam, M., Reichle, R. H., Mishra, U., Zona, D., & Oechel, W. C. (2018). Characterizing permafrost active layer dynamics and sensitivity to landscape spatial heterogeneity in Alaska. *The Cryosphere*, *12*(1), 145–161. https://doi.org/10.5194/tc-12-145-2018

Zona, D., Lafleur, P. M., Hufkens, K., Bailey, B., Gioli, B., Burba, G., Goodrich, J. P., Liljedahl, A. K., Euskirchen, E. S., Watts, J. D., Farina, M., Kimball, J. S., Heimann, M., Göckede, M., Pallandt, M., Christensen, T. R., Mastepanov, M., López-Blanco, E., Jackowicz-Korczynski, M., … Oechel, W. C. (2022). Earlier snowmelt may lead to late season declines in plant productivity and carbon sequestration in Arctic tundra ecosystems. *Scientific Reports*, *12*(1), Article 1. https://doi.org/10.1038/s41598-022-07561-1

Open Science statement

Data and code are publicly available from:

 https://github.com/EliseGallois/Above_v_Below_Phenology

Supplementary Materials

Table S1. Site metadata summaries, including geographical location, soil type, site climate summaries, and vegetation properties.

Site Name	Coordinates (Lat, Lon)		Average July-Aug Surface Temperature (°C)	# Plots (Clusters containing 3 x soil cores)	Vegetation Properties	Milled Peat Type
Kluane Plateau	61.28, 138.93	-	6.8	5	Shrub dominated and mixed-species plots	Golf Green Sphagnum Peat Moss
Toolik Lake	68.63, 149.59	-	14.3	10	Graminoid dominated, shrub dominated, and mixed-species plots	Sunshine Canadian Peat Moss
Niwot Ridge	70.49, 147.29	-	10.8	12	Graminoid dominated, shrub dominated, and mixed-species plots	Golf Green Sphagnum Peat Moss
BC Coastal Mountains	50.04, 123.19	-	7.1	6	Graminoid dominated, shrub dominated, and mixed-species plots	Golf Green Sphagnum Peat Moss + Promix Peat Moss (mixed)
Cairngorms	57.07, -3.49		13.6	6	Shrub dominated and mixed-species plots	Jamieson Brothers Irish Peat Moss
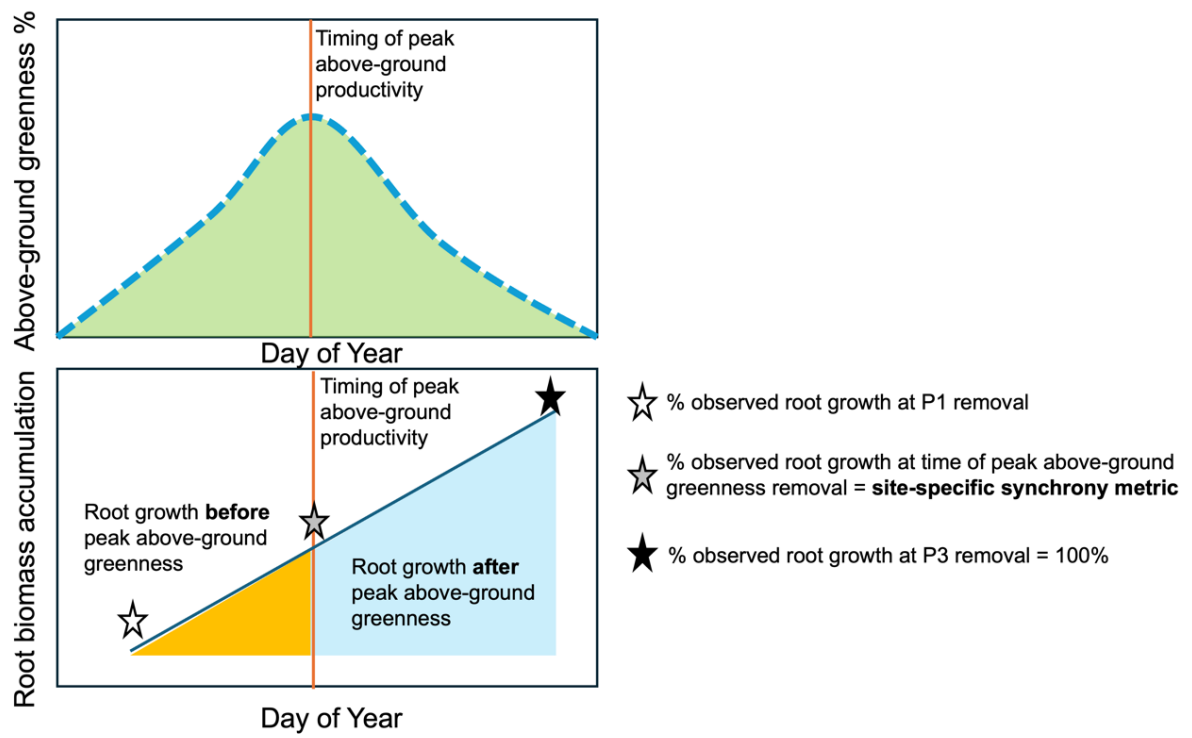
Figure S1. Schematic of the site-specific "synchrony metric" described in the methods and calculated using **Equation 3**.
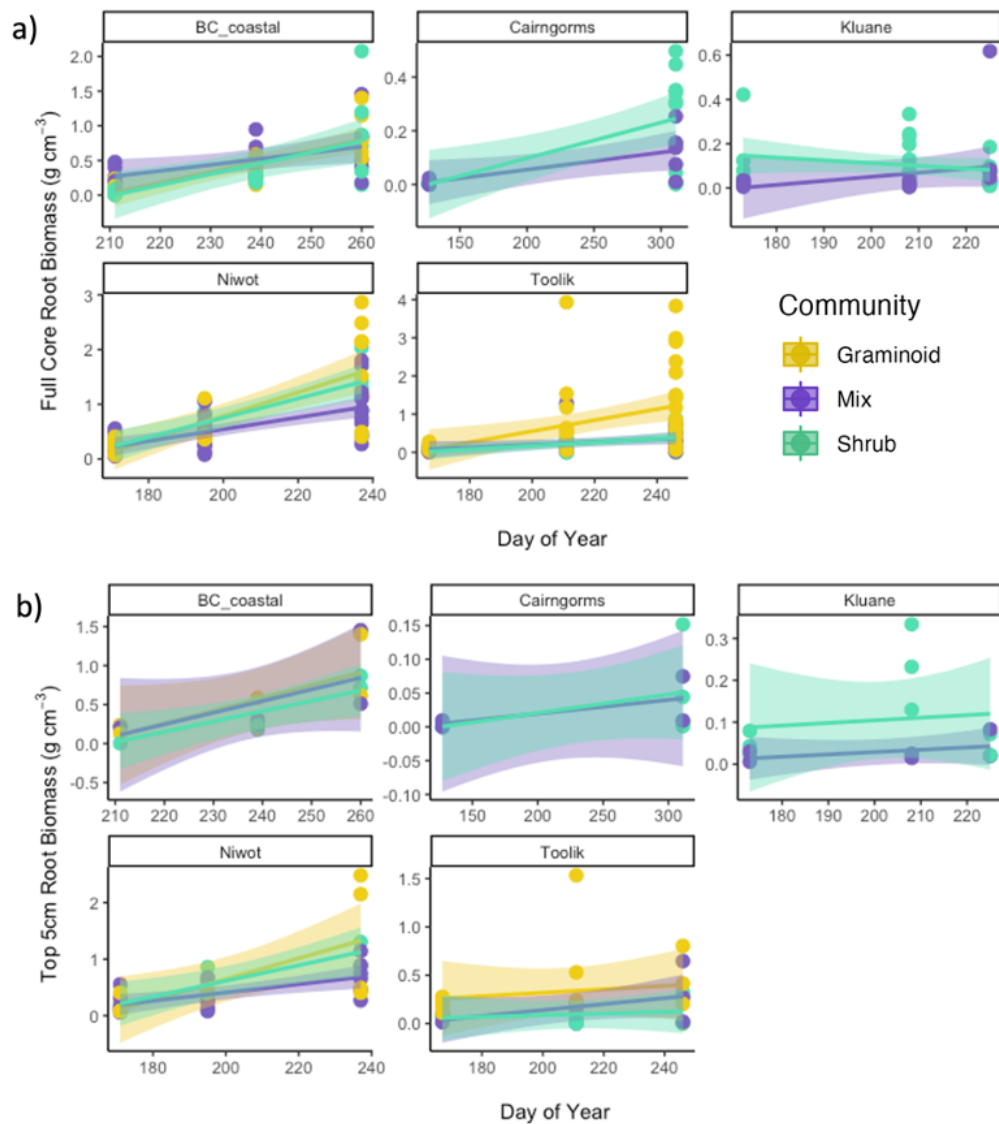
Figure S2. While relative magnitudes of root biomass differ across both data types, the differences between community types at each site remain consistent. Root Biomass accumulation over time categorised by plant community type. Panel (a) includes data calculated from the full length of each core. Panel (b) includes data calculated from only the top 5cm of each core.

1014

1015
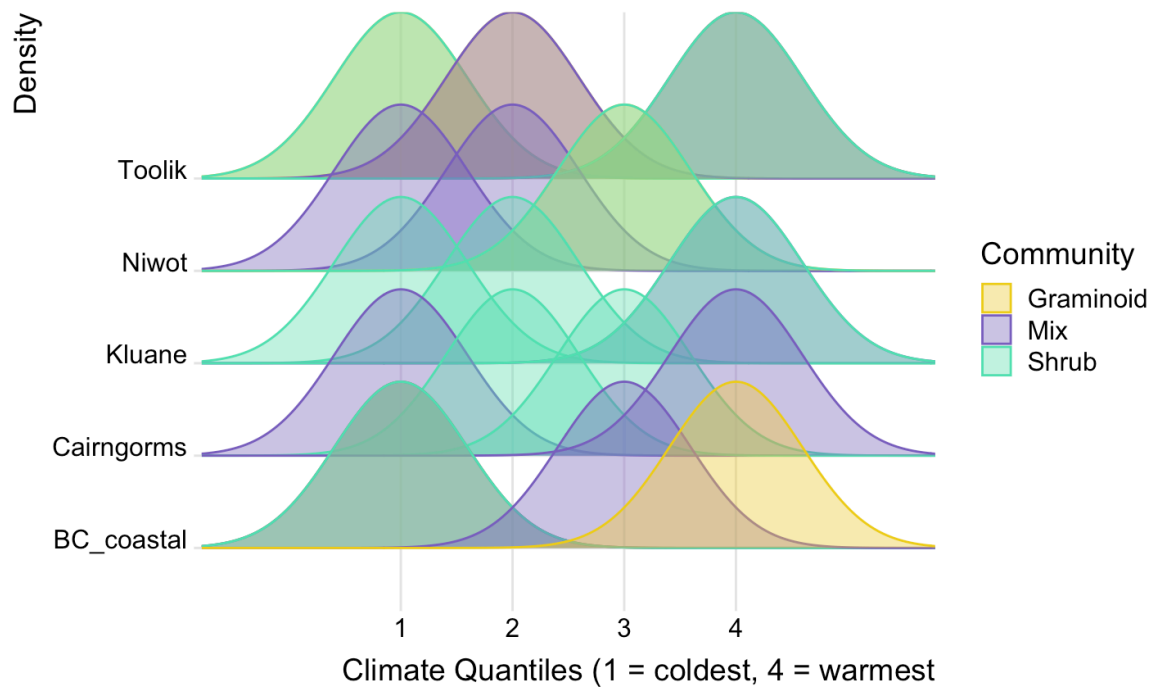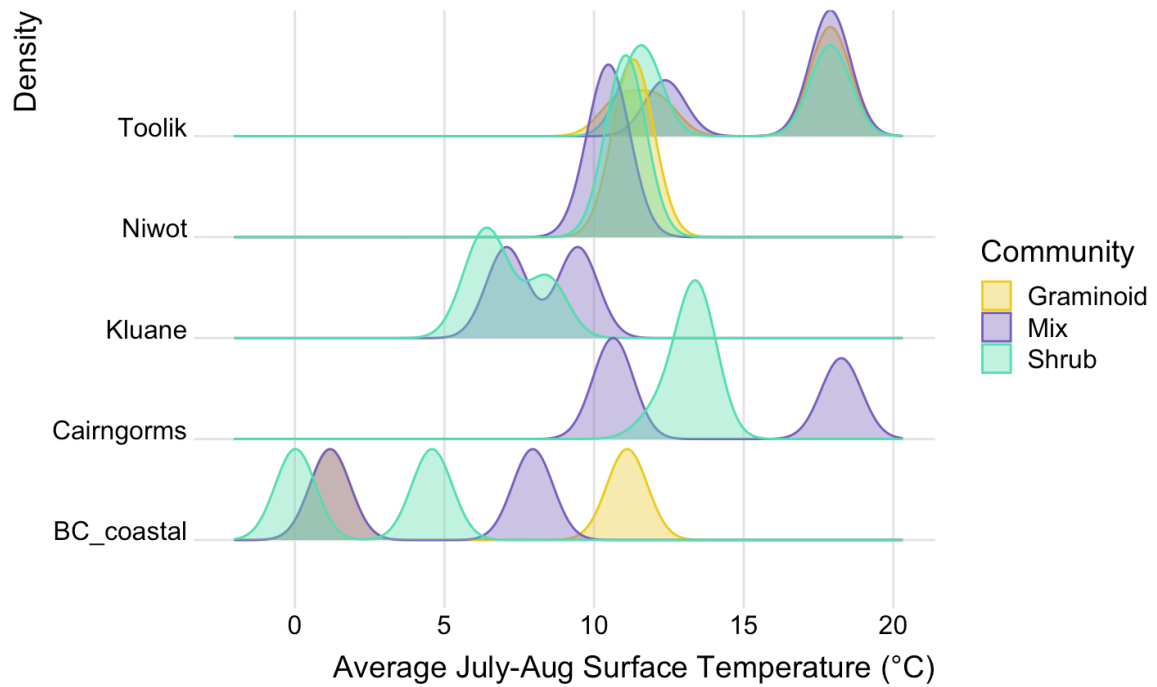
1016 **Figure S3.** Community type and surface temperature do not covary across the sites. Distribution of
1017 summer surface temperatures by site, coloured by community type. In the top panel, climate is
1018 represented by average July-August surface temperature. In the bottom panel, climate is represented by
1019 climate quantile classifications.
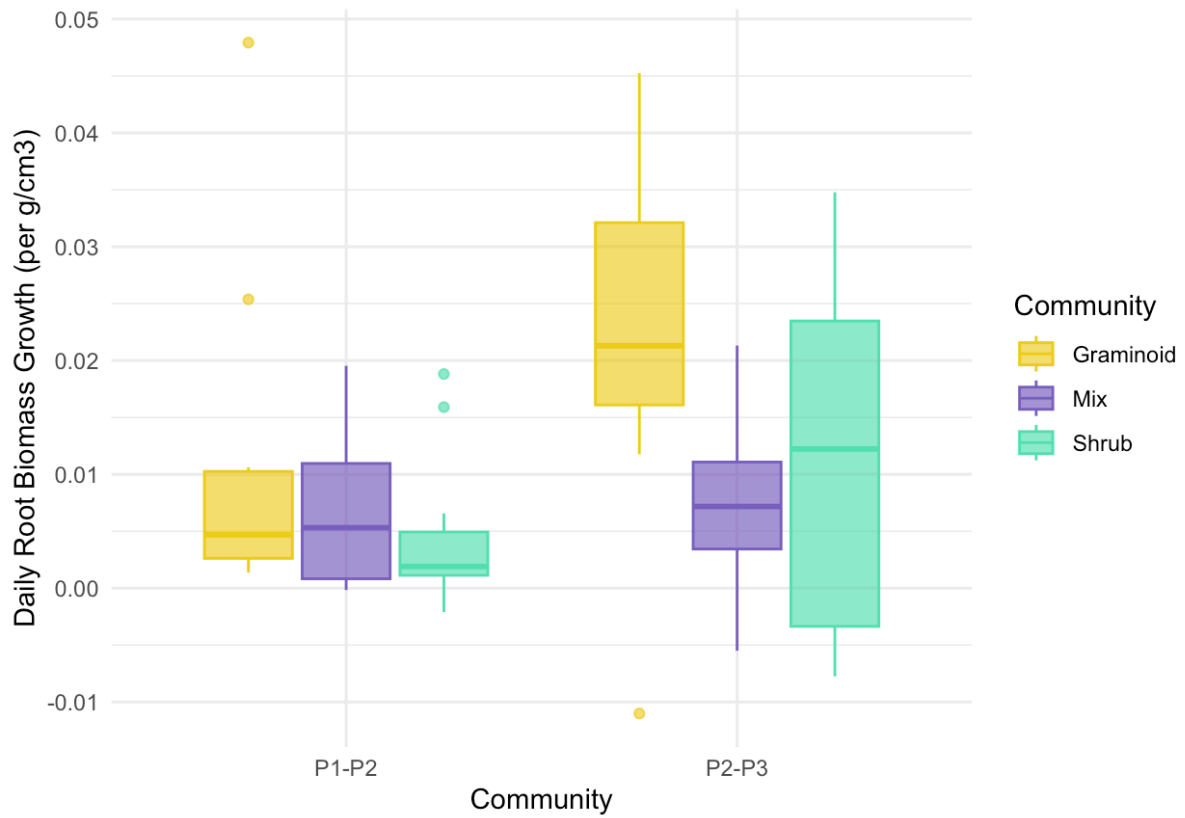
Figure S4: Root growth rate accelerates across all community sites, but especially in graminoid-dominated plots. Daily root growth rates between P1 and P2, and daily root growth rates between P2 and P3 across sites, coloured by community type.

Table S2: Statistical results for the hierarchical Bayesian models relating local surface temperature variation (i.e., climate quantiles 1-4), community type (graminoid, shrub, mix), and phenophase timing (P1, P2, P3, biomass model only) to root biomass, daily root growth rates, and above-vs below-ground asynchrony. These models included 'Site' as a random intercept.

MODEL NAME	TERM	ESTIMATE	STD. ERROR	LOWER 95% CI	UPPER 95% CI
ROOT BIOMASS Versus **TEMPERATURE** and **COMMUNITY** and **PHENOPHASE**	Intercept	0.34	0.14	0.05	0.63
	Community: Mix	-0.14	0.05	-0.24	-0.04
	Community: Shrub	-0.12	0.06	-0.23	-0.02
	Core_ID:P2	0.24	0.04	0.15	0.33
	Core_ID:P3	0.51	0.05	0.42	0.6
	Climate Quantile 2	0.1	0.06	-0.01	0.22
	Climate Quantile 3	0.08	0.06	-0.04	0.21
	Climate Quantile 4	0	0.06	-0.12	0.12
	Site__Intercept	0.26	0.14	0.1	0.66
	sigma	0.19	0.01	0.17	0.23
	Site[BC_coastal,Intercept]	0.1	0.13	-0.17	0.38
	Site[Cairngorms,Intercept]	-0.12	0.14	-0.41	0.15
	Site[Kluane,Intercept]	-0.2	0.14	-0.48	0.06
	Site[Niwot,Intercept]	0.19	0.13	-0.07	0.48
	Site[Toolik,Intercept]	0.03	0.13	-0.24	0.3
ROOT GROWTH RATE Versus **TEMPERATURE** and **COMMUNITY**	Intercept	0.01	0	0	0.02
	Community: Mix	-0.01	0	-0.01	0

	Community: Shrub	-0.01	0	-0.01	0
	Climate Quantile 2	0	0	-0.01	0
	Climate Quantile 3	0	0	0	0.01
	Climate Quantile 4	0	0	-0.01	0
	Site__Intercept	0.01	0	0	0.02
	sigma	0	0	0	0.01
	Site[BC_coastal,Intercept]	0	0	0	0.01
	Site[Cairngorms,Intercept]	-0.01	0	-0.02	0
	Site[Kluane,Intercept]	-0.01	0	-0.01	0
	Site[Niwot,Intercept]	0.01	0	0	0.02
	Site[Toolik,Intercept]	0	0	-0.01	0.01
ROOT SYNCHRONY METRIC Versus TEMPERATURE and COMMUNITY	Intercept	2.1	2.13	-2.14	6.37
	Community: Mix	-5.48	2.05	-9.51	-1.42
	Community: Shrub	0.87	2.05	-3.25	4.88
	Climate Quantile 2	0.8	2.59	-4.28	5.89
	Climate Quantile 3	-1.04	2.25	-5.48	3.37
	Climate Quantile 4	-0.4	2.14	-4.54	3.75
	Site__Intercept	1.17	1.03	0.04	3.71
	sigma	4.65	0.6	3.65	6.02
	Site[BC_coastal,Intercept]	-0.09	1.13	-2.62	2.3
	Site[Cairngorms,Intercept]	0.06	1.14	-2.34	2.61
	Site[Kluane,Intercept]	-0.12	1.13	-2.76	2.22

Site[Niwot,Intercept]	0.34	1.13	-1.76	3.15
Site[Toolik,Intercept]	-0.33	1.15	-3.13	1.69

Table S3: Statistical results for the hierarchical Bayesian models relating local surface temperature variation (i.e., climate quantiles 1-4), and community type (graminoid, shrub, mix), and phenophase timing (P1, P2, P3 -biomass model only) to root biomass, daily root growth rates, and above-vs below-ground asynchrony. These models included 'Site' as a random intercept. These results only include root biomass data from the top 5cm of each core.

Model Name	Term	Estimate	Std. Error	Lower 95% CI	Upper 95% CI
ROOT BIOMASS Versus **TEMPERATURE** and **COMMUNITY** and **PHENOPHASE**	Intercept	0.29	0.16	-0.03	0.61
	Community: Mix	-0.11	0.07	-0.24	0.02
	Community: Shrub	-0.09	0.07	-0.23	0.04
	Core_ID:P2	0.15	0.06	0.04	0.26
	Core_ID:P3	0.33	0.06	0.21	0.44
	Climate Quantile 2	0.07	0.08	-0.08	0.21
	Climate Quantile 3	0.09	0.08	-0.06	0.25
	Climate Quantile 4	0.09	0.08	-0.07	0.23
	Site_Intercept	0.31	0.17	0.12	0.76
	sigma	0.24	0.02	0.21	0.28
	rSite[BCcoastal,Intercept]	0.2	0.15	-0.12	0.52
	rSite[Cairngorms,Intercept]	-0.21	0.15	-0.54	0.09
	rSite[Kluane,Intercept]	-0.16	0.16	-0.51	0.14
	rSite[Niwot,Intercept]	0.21	0.15	-0.09	0.52
	rSite[Toolik,Intercept]	-0.07	0.15	-0.39	0.22
ROOT GROWTH RATE Versus **TEMPERATURE** and **COMMUNITY**	Intercept	0.01	0.01	0	0.02
	Community: Mix	0	0	-0.01	0
	Community: Shrub	0	0	-0.01	0
	Climate Quantile 2	0	0	-0.01	0
	Climate Quantile 3	0.01	0	0	0.01
	Climate Quantile 4	0	0	-0.01	0

	Site_Intercept	0.02	0.03	0	0.09
	sigma	0.01	0	0.01	0.01
	rSite[BCcoastal,Intercept]	0.01	0.01	0	0.02
	rSite[Cairngorms,Intercept]	-0.01	0.01	-0.03	0
	rSite[Kluane,Intercept]	0	0.01	-0.02	0.01
	rSite[Niwot,Intercept]	0	0.01	-0.01	0.01
	rSite[Toolik,Intercept]	0	0.01	-0.02	0.01
ROOT SYNCHRONY METRIC Versus TEMPERATURE & COMMUNITY	Intercept	2.05	3.29	-4.41	8.82
	Community: Mix	-5.55	3.28	-11.98	0.91
	Community: Shrub	1.15	3.35	-5.38	7.79
	Climate Quantile 2	-0.53	4.91	-10.44	9.11
	Climate Quantile 3	-2.4	3.88	-10.18	5.23
	Climate Quantile 4	-0.37	3.01	-6.24	5.56
	Site_Intercept	1.61	1.4	0.06	5.29
	sigma	5.81	0.97	4.28	8.14
	rSite[BCcoastal,Intercept]	-0.03	1.53	-3.39	3.28
	rSite[Cairngorms,Intercept]	0.31	1.64	-2.81	4.32
	rSite[Kluane,Intercept]	-0.04	1.61	-3.62	3.31
	rSite[Toolik,Intercept]	-0.3	1.51	-3.87	2.68